PET adapted lung IMRT

High-resolution pulmonary ventilation and perfusion PET/CT allows for functionally adapted intensity modulated radiotherapy in lung cancer

Shankar Siva [a,b,*], Roshini Thomas [c], Jason Callahan [d], Nicholas Hardcastle [e], Daniel Pham [c], Tomas Kron [a,e], Rodney J. Hicks [a,d], Michael P. MacManus [a,b], David L. Ball [a,b], Michael S. Hofman [a,d]

[a] Sir Peter MacCallum Department of Oncology, University of Melbourne; [b] Division of Radiation Oncology and Cancer Imaging; [c] Department of Radiotherapy Services; [d] Centre for Molecular Imaging; and [e] Department of Physical Sciences, Peter MacCallum Cancer Centre, Australia

ABSTRACT

Background and purpose: To assess the utility of functional lung avoidance using IMRT informed by four-dimensional (4D) ventilation/perfusion (V/Q) PET/CT.
Materials and methods: In a prospective clinical trial, patients with non-small cell lung cancer (NSCLC) underwent 4D-V/Q PET/CT scanning before 60 Gy of definitive chemoradiation. Both "highly perfused" (HPLung) and "highly ventilated" (HVLung) lung volumes were delineated using a 70th centile SUV threshold, and a "ventilated lung volume" (VLung) was created using a 50th centile SUV threshold. For each patient four IMRT plans were created, optimised to the anatomical lung, HPLung, HVLung and VLung volumes, respectively. Improvements in functional dose volumetrics when optimising to functional volumes were assessed using mean lung dose (MLD), V5, V10, V20, V30, V40, V50 and V60 parameters.
Results: The study cohort consisted of 20 patients with 80 IMRT plans. Plans optimised to HPLung resulted in a significant reduction of functional MLD by a mean of 13.0% (1.7 Gy), $p = 0.02$. Functional V5, V10 and V20 were improved by 13.2%, 7.3% and 3.8% respectively (p-values < 0.04). There was no significant sparing of dose to functional lung when adapting to VLung or HVLung. Plan quality was highly consistent with a mean PTV D95 and D5 ranging from 60.8 Gy to 61.0 Gy and 63.4 Gy to 64.5 Gy, respectively, and mean conformity and heterogeneity index ranging from 1.11 to 1.17 and 0.94 to 0.95, respectively.
Conclusion: IMRT plans adapted to perfused but not ventilated lung on 4D-V/Q PET/CT allowed for reduced dose to functional lung whilst maintaining consistent plan quality.

© 2015 Elsevier Ireland Ltd. All rights reserved. Radiotherapy and Oncology 115 (2015) 157–162

Damage to normal pulmonary tissues is a recognised dose-limiting toxicity associated with localised irradiation of non-small cell lung cancer (NSCLC). Pneumocytes and the vascular endothelium are considered to be the most radiation sensitive tissues in the lungs [1]. Complex inflammatory molecular responses to ionising radiation in these tissues result in both bronchoalveolar fibrosis and vascular endothelial effects, which can cause pulmonary ventilation and perfusion deficits [2]. Imaging modalities capable of assessing ventilatory function and blood perfusion have demonstrated that these deficits can be observed and are associated with the clinical risk of toxicity [3–6]. Planar scintigraphy

using ^{99m}Tc-labelled macroaggregated albumin (MAA) is a long-established imaging standard for functional ventilation/perfusion evaluation. Single positron emission computed tomography (SPECT), and the subsequent advent of hybrid SPECT/CT devices have improved diagnostic accuracy by enabling anatomic characterisation of scintigraphic abnormalities [7]. These imaging modalities can be used to identify the most functional areas of the lung and facilitate avoidance of these regions. Perfusion SPECT/CT has been demonstrated to allow for functional lung avoidance during lung radiotherapy planning by several groups [8–10]. Recently, ventilation SPECT/CT has also been explored as a potential tool for functional lung avoidance by Munawar et al. [11].

PET/CT offers a further opportunity to improve the image quality and accuracy of contemporary functional lung imaging [12].

Our group has demonstrated superior sensitivity of PET in the detection of radioactive substances, respiratory gating capability, and both higher spatial and temporal resolution [13,14]. Unlike SPECT/CT, PET/CT is fully quantitative. Additionally, respiratory gating (4D) allows for accurate attenuation correction which improves imaging accuracy and allows for accurate anatomical co-registration [13]. The purpose of this study is to assess the utility of radiotherapy optimisation to functional lung volumes using state-of-the-art gated V/Q-PET/CT acquisition technology. The study population consists of patients with NSCLC receiving definitive radiotherapy undergoing pre-treatment four-dimensional (4D) V/Q PET/CT. The primary hypothesis is that dose to functional regions of the lung can be reduced through adaptation of radiotherapy plans optimised to these functional volumes. In this study, both perfusion and ventilation datasets are acquired contemporaneously allowing for comparison of the value of either modality in functionally adaptive planning. As radiotherapy plan quality can dramatically impact dosimetric evaluation, particular attention is paid to a rigorous intensity modulated radiotherapy (IMRT) planning methodology.

Material and methods

Patient selection

This work was part of an observational prospective clinical trial (Universal Trial Number U1111-1138-4421) of patients undergoing curative intent radiotherapy for NSCLC. This study received institutional review board approval by the Peter MacCallum Cancer Centre. All patients had pre-treatment pulmonary function testing (PFTs) with testing for diffusing capacity of the lung for carbon monoxide (DLCO). All patients were planned to receive 60 Gy in 30 fractions of external beam radiotherapy, 5 fractions per week with or without concurrent chemotherapy using a departmental cone-beam CT image guidance protocol.

4D Ventilation/perfusion PET/CT acquisition

All scans were performed on a GE-Discovery™ 690 PET/CT scanner (GE Medical Systems Milwaukee, Wisconsin, USA). 4D V/Q PET/CT technique and acquisition protocol was performed as previously described in detail by our group [13,14]. In brief, ventilation imaging was performed following inhalation of Galligas, produced by substituting Gallium-68 instead of Technetium-99 m in a Technegas generator (Cyclomedica, Australia). Approximately 200 MBq of Galligas was added to the carbon crucible prior to inhalation. The patients were positioned supine on the PET/CT scanner in a default planning position using the radiotherapy palette and head rest with their arms raised. The patient breathing trace was tracked using the Varian RPM™ respiratory tracking system (Varian Medical Systems, Palo Alto, California). The patients were instructed to breathe freely for the duration of the scans. A contemporaneous low-dose chest 4D-CT acquisition was performed using 125 kVp energy photons at 10 mA and a slice thickness of 5 mm. The field of view for both 4D-PET and 4D-CT encompassed the entire lung fields. Ventilation-PET scan of the lungs was acquired (2 bed positions, 5 min per bed). Approximately 40 MBq of ^{68}Ga-MAA was subsequently administered intravenously, and 4D Perfusion-PET acquired over the same field-of-view (2 bed positions, 5 min per bed). The ventilation and perfusion PET scans were reconstructed as both gated and un-gated images. Phase matched attenuation correction with 5 and 10 respiratory bins was used to reconstruct the 4D-PET/CT scan. The free-breathing PET acquisition was subsequently co-registered with the average intensity projection of the 4D CT. Fig. 1 shows typical images for ventilation and perfusion scans.

4DCT simulation

Patients were simulated supine with arms located above the head and a bolster under the knees for comfort. A time resolved 4D CT scan for Radiotherapy planning purposes was performed on all patients using a 64-slice Big Bore Brilliance™ CT scanner (Koninklijke Philips Electronics, Amsterdam, The Netherlands). The pressure sensitive belt (Philips Bellows system) was used for respiratory-sorting and data binned into 10 phases for image reconstruction. The patients were scanned in helical mode, using 140 kVp, 3-mm slice thickness, 3-mm increment and 0.44-s rotation time. Images were reconstructed with ~3.5 mm^3 voxel resolution (3-mm slice thickness × 1.0742-mm pixel spacing).

Volume marking/tumour delineation

From the respiratory-sorted imaging phases of the Radiotherapy planning scan, average (AVG) and maximum intensity projection (MIP) series were reconstructed. Target delineation was performed on an Elekta FocalSim™ (Crawley, UK) workstation. Standardised lung window/level settings (1700/−300) were used in the MIP image series. All volumes were delineated onto the AVG CT dataset for final dose calculation. An internal target volume (ITV) was delineated from the MIP series, with a further isotropic expansion of 5 mm used to generate the clinical target volume (CTV). A further 10 mm isotropic expansion from CTV was used to create the planning target volume (PTV). The anatomical lung volume was delineated using the planning CT dataset. A highly perfused lung volume (HPLung) and highly ventilated lung volume (HVLung) were delineated using a visually adapted 70th centile SUV threshold method, as recently described by our group [15,16] and others [17]. It was apparent that HVLung was considerably smaller than HPLung, so a ventilated lung volume (VLung) was created to approximate the HPLung volume using the 50th centile SUV threshold, a methodology previously reported by Munawar et al. [11]. Any clumping of Galligas was excluded from the volume using the method described by Kipritidis et al. [18], by which an upper threshold was set that removed voxels >4 standard deviations above the mean. Radiotherapy planning was completed on the 4D simulation dataset by employing a rigid registration method of image fusion with the 4D V/Q scans, allowing contours to be accurately transferred between the datasets. For each of the lung volumes, the organ at risk (OAR) for planning purposes was defined as the volume of both lungs minus the volume of the GTV.

Planning technique

A single qualified radiotherapy planner created a total of 80 IMRT plans for the anatomical, HP, HV and V lung volumes. Each plan was optimised using the planning 4DCT AVG dataset to the relevant lung volume, without being informed by the alternative lung volumes. Inverse IMRT planning was performed for each patient using Varian Eclipse treatment planning software (v11, Palo Alto, California USA). A 2.5 mm calculation grid was used to perform the dose calculation using an analytic anisotropic algorithm (AAA V.11.0.21). A sliding window IMRT technique was employed to prescribe 60 Gy to cover 95% of the PTV using 5–6 coplanar 6MV X-ray beams. The same beam arrangements were used in all four-treatment plans. Beam arrangements were defined by the position of the tumour volume, with the aim of limiting beam paths through the contralateral lung and without consideration of functional lung geometry. The organs at risk (OARs) optimised in the inverse planning process included; bony spinal canal, oesophagus, heart, as well as the lung volume relevant to each plan. A summary of the target volume and OARs as well as
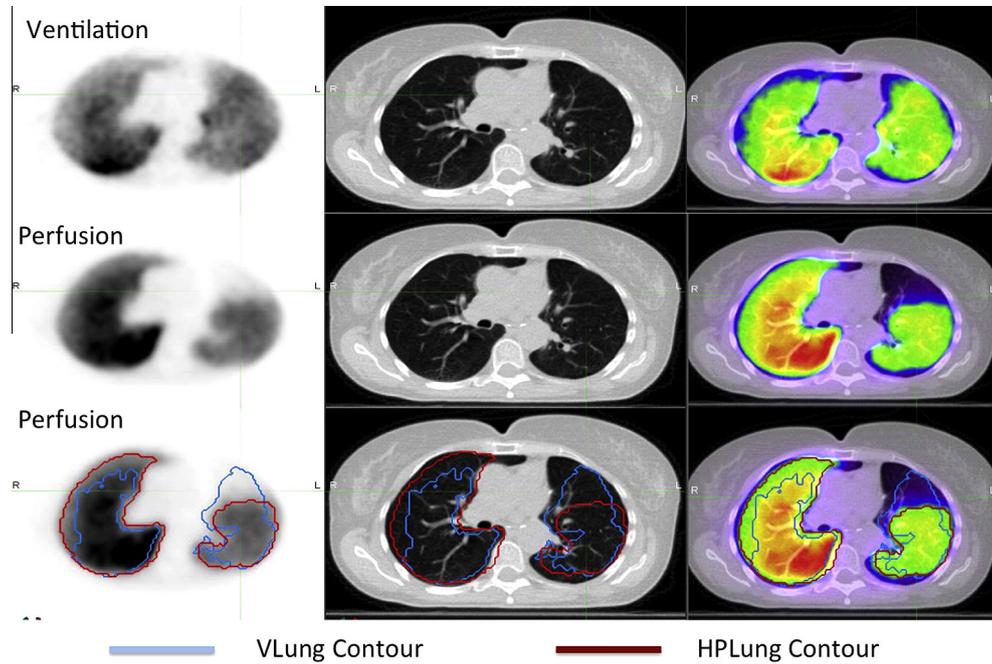
Fig. 1. V/Q PET/CT scan in a patient with emphysema. PET images are displayed in the first column, co-registered PET/CT images in the second column showing both ventilation images (top row) and perfusion images (bottom row). There is markedly more artefact in the ventilation images with clumping of tracer in central airways.

Table 1
Summary of the target volume, organs at risk and IMRT priorities.

Structure	Metric	Anatomical plan		Functional plans	
		Tolerance	Priority	Tolerance	Priority
PTV	V60	⩾95%	80–85	⩾95%	80–85
Bony SC	Max dose (0.03 cc)	⩽50 Gy	55–80	⩽50 Gy	55
Lung	Mean	<20 Gy	50–60		
	V30	<30%	55–60		
	V20	<35%	55–65		
	V5	<60%	60–65		
Functional lung	Mean			<20 Gy	50–60
	V30			<30%	55–60
	V20			<35%	55–65
	V5			<60%	60–65
Oesophagus	Max dose (0.03 cc)	<63 Gy	55–65	<63 Gy	55–65
	Mean	<34 Gy	50	<34 Gy	50
Heart	V40	<35%	40–50	<35%	40–50
	Mean	<30 Gy	40–50	<30 Gy	40–50
	Max dose (0.03 cc)	<70 Gy	50	<70 Gy	50
Brachial plexus	Max dose (0.03 cc)	<63 Gy	45	<63 Gy	45
Normal tissue objective			75		75

the parameters used in the normal tissue objective function can be seen in Table 1. The information summarised in this table is representative of the consistency achieved between IMRT plans, as it indicates the starting point for each plan. The first plan was optimised solely to anatomical lung. Subsequent IMRT plans were optimised to the HPLung, HVLung and VLung functional volumes. Although the plans to functional lung did not include optimisation constraints to the conventional anatomical lung volumes, it was ensured that all plans still met the anatomical lung constraints of mean lung dose (MLD) <20 Gy, V5 < 60%, V20 < 35%, V30 < 30% employed at our institution. Dose–volume histogram (DVH) parameters for functional volumes are designated $f_{HP}DVH$, $f_{HV}DVH$ and $f_{V}DVH$, referring to the highly perfused, highly ventilated and ventilated lung, respectively.

Plan optimisation strategy

The planning strategy employed starting priorities and dose constraints as indicated in Table 1. For plans where it was evident that one of the OARs such as cord or oesophagus was in close proximity to the target volume, priorities were increased from the onset to approach PTV objectives, which were in the order of 80 (upper objective) to 85 (lower objective). The main planning goal was to achieve prescription dose to 95% of the PTV, and limit toxicity to the spinal cord and oesophagus. No plan resulted in compromise of OAR dose limits. The lung volume relevant to each plan was optimised to the best plan possible until another dose limiting structure neared tolerance, or PTV coverage or conformity was compromised. This was done via manual manipulation of the DVH during IMRT iterations, lowering the acceptable tolerances by 5–10 Gy each time. Plan quality was furthermore evaluated through evaluation of conformity indices and heterogeneity indices.

The heterogeneity index (HI) was given by the formula based on that of Murshed et al. [19];

$$HI = \frac{D_{95\%}}{D_{5\%}}$$

where D95 represents the dose received by 95% of the PTV volume, and D5 represents the dose received by 5% of the PTV volume.

The conformity index (CI) was given by the formula based on Shaw et al. [20]

$$CI = PIV/TV$$

where PIV (Prescription Isodose Volume) represents the volume receiving 60 Gy, and TV (Target Volume) represents the PTV.

Statistical analyses

The anatomical, HPLung, HVLung and VLung volumes were compared using repeated measures ANOVA. Lung volumes were tested for mutual association using a Pearson correlation statistic. The following anatomical and functional volumetric parameters
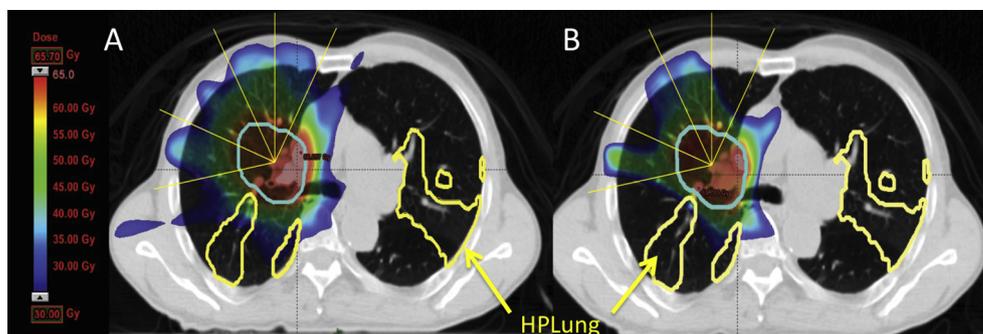
Fig. 2. Axial dose colour wash of a patient with severe emphysema showing a conventional IMRT plan optimised to anatomical lung (A), and a functionally adapted plan optimised to the HPLung volume (B), demonstrating differences in dose distribution that may be observed due to functional dose painting.

were compared using multiple paired *t*-tests for MLD, V5, V10, V20, V30, V40, V50 and V60. For each volumetric parameter, the mean difference in functional lung dose between conventional IMRT planning and functionally adapted IMRT planning was described for the relevant functional lung volume. Mean differences, standard errors and their respective confidence intervals were reported. Plan quality was assessed through repeated measures ANOVA testing for each of PTV volume coverage, plan heterogeneity and conformity. All multiple comparisons tests were corrected using the Holm–Sidak method. Statistical significance was defined as P < 0.05 using a 2-tailed test. All analyses were performed using PRISM v6.0.

Results

Patient characteristics and lung volumes

Between December-2011 and June-2013, 20 patients with NSCLC participated in this prospective study. Patient characteristics and lung volumetrics are outlined in Supplementary Table S1. There were two patients who presented with synchronous solitary isolated brain metastasis who underwent resection and subsequent definitive thoracic irradiation. The most common tumour location was the right upper lobe (*n* = 11). The mean (±SD) PTV volume was 400 cc (±265 cc), and conventional anatomical lung volume was 3720 cc (±1043 cc). The mean volumes for HPLung and VLung (±SD) were similar at 1876 cc (±677 cc) and 1904 cc (±505 cc), respectively. The mean volume (±SD) of HVLung was 932 cc (±258 cc), which was significantly smaller than the HPLung volume by a mean of 943 cc (*p* < 0.01). The distribution of tracer uptake appeared to qualitatively suggest that more patients had large areas of perfusion deficits as compared to those with large ventilation defects. The ratio of functional lung to anatomical lung volume was consistent, with a mean (±SD) ratio of 0.255 (±0.035) for HVLung and 0.520 (±0.066) for VLung. This ratio varied to a greater extent in HPLung at 0.540 (±0.207). This resulted in good correlation between the anatomical lung and ventilated lung volumes within patients, Pearson *r* = 0.832, *p* < 0.01 and *r* = 0.856, *p* < 0.01 for HVLung and VLung, respectively. However, there was poor correlation between anatomical lung and HPLung volumes, Pearson *r* = 0.027, *p* = 0.49. Fig. 2a and 2b demonstrates a representative perfusion PET/CT in a patient with severe emphysema, showing the original plan used for treatment based on the anatomical lung and a plan optimised to account for large deficits observed in areas of perfused lung.

Doses to functional lung

IMRT planned to the anatomical lung volumes blinded to the findings of the perfusion PET/CT resulted in no significant

differences in MLD in either f$_{HP}$DVH, f$_{HV}$DVH or f$_V$DVH. The mean (±SD) anatomical MLD was 13.4 Gy (±3.12 Gy), compared to 13.1 Gy (±2.39 Gy) for HPLung (*p* = 0.83), 12.7 Gy (±3.0 Gy) for VLung (*p* = 0.21), and 12.1 Gy (±3.97 Gy) for HVLung (*p* = 0.21). IMRT planned to conventional anatomical lung volumes demonstrated a small but statistically significant reduction in f$_V$DVH V40–V60 parameters and the f$_{HP}$DVH V60 parameter (at a detriment to the f$_{HP}$DVH) [Supplementary Table S2]. IMRT lung planning optimised to avoid regions of HPLung resulted in improved dose volumetric outcomes to functioning lung. The f$_{HP}$DVH MLD was reduced by a mean of 13.0% (1.7 Gy), *p* = 0.03, when adapting the plan to the functional HPLung volume (Supplementary Table S3). This adapted plan also resulted in significant reductions of dose across the f$_{HP}$DVH V5, V10 and V20 parameters, which were improved by 13.2%, 7.3% and 3.8% respectively (*p*-values < 0.035), Fig. 3. By contrast, IMRT plans adapted to HVLung and VLung did not demonstrate any significant improvement to either the f$_{HV}$DVH or f$_V$DVH MLD, or any of the other functional DVH parameters assessed (Supplementary Tables S4 and S5). Improvements in f$_{HP}$DVH MLD and V5–V20 were all independent of PTV volume (Spearman *r* range 0.056–0.389, all *p*-values > 0.1).

Assessment of plan quality and doses to OARs

PTV coverage for each plan was compared through analysis of near minimum (D95) and near maximum (D5) doses. The mean PTV D95 was 61.0 Gy for the anatomical lung IMRT plans, whilst each of the HPLung, HVLung and VLung IMRT plans had a mean D95 of 60.8 Gy, (*p* = 0.73). The mean PTV D5 was 63.7 Gy for the anatomical lung IMRT plans. Mean HVLung and VLung PTV D5 values were similar, at 63.4 Gy and 63.3 Gy, respectively, with HPLung marginally higher at 64.5 Gy (*p* = 0.01). Similarly, the conformity and heterogeneity indices were similar between each plan, with a mean (±SD) HI ranging from 0.94 (±0.01) to 0.95 (±0.01), and CI ranging from 1.11 (±0.08) to 1.17 (±0.07). The maximum dose OARs were similar between plans, ranging between a mean of 53.1 Gy and 53.7 Gy for oesophagus (*p* = 0.75) and between a mean of 53.3 Gy and 54.3 Gy for the heart (*p* = 0.59). The spinal canal maximum dose was slightly worse for the HPLung plan at a mean of 38.7 Gy, which was higher than the anatomical, HVLung and VLung plans which ranged between a mean of 35.7 Gy and 36.3 Gy (*p* = 0.01). The ratio between the functionally adapted IMRT plans to the anatomical IMRT plans in terms of plan quality indices and maximum dose to OARs is described in Fig. 4.
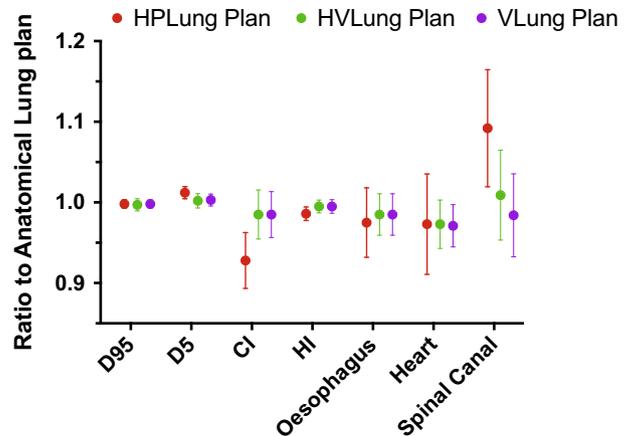
Discussion

In this study we demonstrate that functionally adapted planning using 4D-V/Q PET/CT can be used to inform IMRT planning to reduce dose to functional regions of the lung. Plans optimised
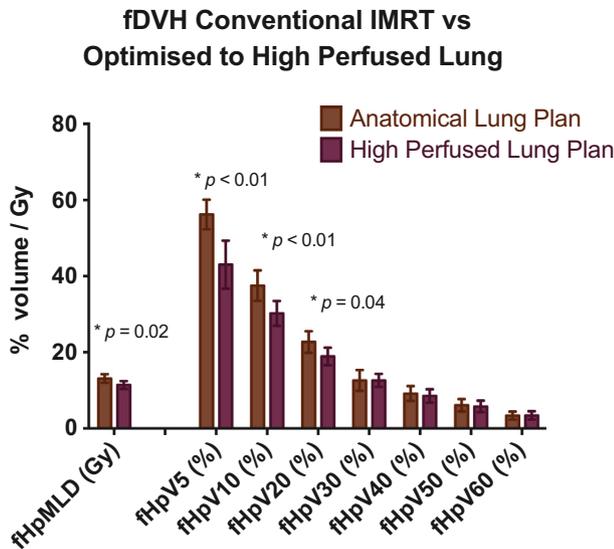
Fig. 3. Comparison of conventional anatomical plan versus plan adapted to HPLung assessing functional f$_{HP}$DVH parameters.

Fig. 4. Ratio of plan quality indices and dose to organs at risk for the conventional IMRT plan to the IMRT plan optimised to each functional lung volume. Mean (±95% CIs) ratio is presented.

to the functional lung volume did not incur a penalty when assessing conventional anatomical lung volumetrics. When planning to the functional lung volume using our methodology there was minimal detriment to plan quality in terms of (a) coverage of target (b) plan quality and (c) dose to OARs. An underlying assumption of this work is that preferential sparing of well ventilated and perfused lung compared to poorly ventilated and perfused lung will facilitate better long-term preservation of global pulmonary function after definitive lung radiotherapy. Certainly, dose-dependent loss in pulmonary ventilation and perfusion has been previously observed using V/Q SPECT [21–23]. In this study, statistically significant reductions in dose to perfused lung were demonstrated in the f$_{HP}$DVH MLD by 13.0%, and the V5, V10 and V20 dose regions by 13.2%, 7.3% and 3.8%, respectively. Demonstrated functional dose reductions were independent of PTV volume. These dose regions are particularly relevant, as these dose regions have been demonstrated to be clinically associated with risk of toxicity when applied to the conventional anatomical lung volume [24]. High dose regions (V30–V60) were not significantly reduced, as these regions were close to the target volume and improvement in functional lung sparing would compromise target coverage and/or plan quality. However, similar reductions of dose to clinically relevant ventilated lung volumes were not possible. This was despite the use of robust and uniform planning techniques applied across both the ventilated and perfused datasets. Additionally, no benefit was seen despite the investigation of two different methodologies to generate clinically equivalent functional volumes to the perfusion dataset – a volume generated using a similar SUVmax threshold and a second volume generated to approximate the physical volume of the perfused lung. Qualitatively, it was apparent that the VLung volume generated using the 50th centile SUV threshold (as previously reported by Munawar et al. [11]) resulted in numerous small islands of volume throughout the lung rather than one contiguous volume, which limited the capacity for functional adaptation of radiotherapy.

We hypothesise that image quality is a major driving factor in the disparity between the capacity for functional dose improvement in perfusion versus ventilation PET. There is more noise in the ventilation images owing to significantly lower activity in the lungs with ventilation compared to perfusion. Furthermore, 'artifacts' from clumping in the proximal airways in patients with airways disease typical in a NSCLC cohort, can result in suboptimal image quality (Fig. 1). These factors contribute to a more inhomogeneous distribution of apparent tracer uptake and camera acquisition that may limit the utility of this technique for precision 'functional dose painting' of lung radiotherapy using IMRT techniques. A corollary can be observed in SPECT/CT literature addressing functional lung avoidance. Recently, ventilation SPECT/CT has been demonstrated to allow modest reductions in dose to ventilated lung by Munawar et al. [11]. However, ventilation SPECT/CT imaging is a similarly technically challenging modality in which to perform radiotherapy optimisation due to relatively poor spatial image resolution and potential clumping of the aerosolised tracer. Furthermore, in this study we found that ventilated functional lung volumes correlated well with CT defined anatomical lung (Pearson r-values > 0.8, p-values < 0.01), which suggests that opportunities to optimise advantage of ventilation mismatches in anatomical versus functional lung may be limited. These factors may explain the relative paucity of the SPECT ventilation literature in comparison to SPECT perfusion with respect to radiotherapy functional lung avoidance.

Our results are consistent with previous reports of IMRT avoidance of perfused lung using older SPECT/CT technology. A previous study of 16 patients by Shioyama et al. using SPECT/CT [25] optimised lung plans on the 50th and 90th percentile of the functional lung and showed that the mean functional lung dose could be reduced by 2.2 Gy and 4.2 Gy respectively. In contrast to our study, these authors reported that functionally adapted plans resulted in reduced coverage of the PTV minimum dose. This is likely to be due to the DVH constraints used. McGuire et al. [26] demonstrated in 5 patients that IMRT adapted to perfused lung could reduce the V20 and V30 to functional lung by a mean 13.7% and 10.6%, respectively. The strength of our study in the context of previous literature is the use of higher resolution respiratory gated PET imaging to accurately define functional lung regions for IMRT planning, and the use of stringent plan quality assessment measures. A potential weakness of our study is the relatively low anatomical mean MLD at 13.4 Gy in our patient population that may have resulted in reduced opportunity to spare dose and underestimate the potential improvement of dose to functional lung. However, there was no bias from patient selection due to target volume in this study as these patients were consecutively enrolled into this prospective study. Our study suggests that IMRT planning optimised to perfused but not ventilated lung volumes allow for reduction in dose to functional lung. This may lead to a potential reduction in respiratory toxicity in patients undergoing definitive

lung radiotherapy. These results should be further validated by other groups using V/Q PET/CT technology.

Conflicts of interest notification

None of the authors have any conflicts of interest to declare in this work.

Role of the funding source

Appendix A. Supplementary data

Supplementary data associated with this article can be found, in the online version, at http://dx.doi.org/10.1016/j.radonc.2015.04.013.

References

[1] Hill R. Radiation effects on the respiratory system. Br J Radiol 2005:75–81.
[2] Tsoutsou PG, Koukourakis MI. Radiation pneumonitis and fibrosis: mechanisms underlying its pathogenesis and implications for future research. Int J Radiat Oncol Biol Phys 2006;66:1281–93.
[3] Zhang J, Ma J, Zhou S, et al. Radiation-induced reductions in regional lung perfusion: 0.1-12 year data from a prospective clinical study. Int J Radiat Oncol Biol Phys 2010;76:425–32.
[4] Yuan ST, Frey KA, Gross MD, et al. Changes in global function and regional ventilation and perfusion on SPECT during the course of radiotherapy in patients with non-small-cell lung cancer. Int J Radiat Oncol Biol Phys 2012;82:e631–8.
[5] Marks LB, Munley MT, Bentel GC, et al. Physical and biological predictors of changes in whole-lung function following thoracic irradiation. Int J Radiat Oncol Biol Phys 1997;39:563.
[6] Hoover DA, Reid RH, Wong E, et al. SPECT-based functional lung imaging for the prediction of radiation pneumonitis: a clinical and dosimetric correlation. J Med Imaging Radiat Oncol 2014;58:214–22.
[7] Roach PJ, Gradinscak DJ, Schembri GP, Bailey EA, Willowson KP, Bailey DL. SPECT/CT in V/Q scanning. Seminars in nuclear medicine, 40. Elsevier; 2010. pp: 455–466.
[8] Christian JA, Partridge M, Nioutsikou E, et al. The incorporation of SPECT functional lung imaging into inverse radiotherapy planning for non-small cell lung cancer. Radiother Oncol 2005;77:271–7.
[9] Lavrenkov K, Christian JA, Partridge M, et al. A potential to reduce pulmonary toxicity: the use of perfusion SPECT with IMRT for functional lung avoidance in radiotherapy of non-small cell lung cancer. Radiother Oncol 2007;83:156–62.
[10] Seppenwoolde Y, Engelsman M, De Jaeger K, et al. Optimizing radiation treatment plans for lung cancer using lung perfusion information. Radiother Oncol 2002;63:165–77.
[11] Munawar I, Yaremko BP, Craig J, et al. Intensity modulated radiotherapy of non-small-cell lung cancer incorporating SPECT ventilation imaging. Med Phys 2010;37:1863–72.
[12] Hicks RJ, Hofman MS. Is there still a role for SPECT–CT in oncology in the PET–CT era? Nat Rev Clin Oncol 2012;9:712–20.
[13] Callahan J, Hofman MS, Siva S, et al. High-resolution imaging of pulmonary ventilation and perfusion with 68Ga-VQ respiratory gated (4-D) PET/CT. Eur J Nucl Med Mol Imaging 2014;41:343–9.
[14] Hofman MS, Beauregard JM, Barber TW, Neels OC, Eu P, Hicks RJ. 68Ga PET/CT ventilation-perfusion imaging for pulmonary embolism: a pilot study with comparison to conventional scintigraphy. J Nucl Med 2011;52:1513–9.
[15] Siva S, Devereux T, Hardcastle N, et al. Feasibility of IMRT planning to reduce dose to functional lung using respiratory gated (4D) gallium-68 Perfusion PET/CT. Int J Radiat Oncol Biol Phys 2014;90:S618–9.
[16] Siva S, Callahan J, Kron T, et al. A prospective observational study of Gallium-68 ventilation and perfusion PET/CT during and after radiotherapy in patients with non-small cell lung cancer. BMC cancer 2014;14:740.
[17] Meng X, Frey K, Matuszak M. Changes in functional lung regions during the course of radiation therapy and their potential impact on lung dosimetry for non-small cell lung cancer. Int J Radiat Oncol Biol Phys 2014;89:145–51.
[18] Kipritidis J, Siva S, Hofman MS, Callahan J, Hicks RJ, Keall PJ. Validating and improving CT ventilation imaging by correlating with ventilation 4D-PET/CT using 68Ga-labeled nanoparticles. Med Phys 2014;41:011910.
[19] Murshed H, Liu HH, Liao Z, et al. Dose and volume reduction for normal lung using intensity-modulated radiotherapy for advanced-stage non–small-cell lung cancer. Int J Radiat Oncol Biol Phys 2004;58:1258–67.
[20] Shaw E, Kline R, Gillin M, et al. Radiation Therapy Oncology Group: radiosurgery quality assurance guidelines. Int J Radiat Oncol Biol Phys 1993;27:1231–9.
[21] Theuws JCM, Kwa SLS, Wagenaar AC, et al. Prediction of overall pulmonary function loss in relation to the 3-D dose distribution for patients with breast cancer and malignant lymphoma. Radiother Oncol 1998;49:233–43.
[22] Boersma LJ, Damen EMF, de Boer RW, et al. Estimation of overall pulmonary function after irradiation using dose-effect relations for local functional injury. Radiother Oncol 1995;36:15–23.
[23] Scheenstra AEH, Rossi MMG, Belderbos JSA, Damen EMF, Lebesque JV, Sonke J-J. Local dose–effect relations for lung perfusion post stereotactic body radiotherapy. Radiother Oncol 2013;107:398–402.
[24] Graham MV, Purdy JA, Emami B, et al. Clinical dose–volume histogram analysis for pneumonitis after 3D treatment for non-small cell lung cancer (NSCLC). Int J Radiat Oncol Biol Phys 1999;45:323–9.
[25] Shioyama Y, Jang SY, Liu HH. Preserving functional lung using perfusion imaging and intensity-modulated radiation therapy for advanced-stage non-small cell lung cancer. Int J Radiat Oncol Biol Phys 2007;68:1349–58.
[26] McGuire S, Marks L, Yin F, Das S. A methodology for selecting the beam arrangement to reduce the intensity-modulated radiation therapy (IMRT) dose to the SPECT-defined functioning lung. Phys Med Biol 2010;55:403.